Journal of Catalysis 309 (2014) 362–375

Contents lists available at ScienceDirect

Journal of Catalysis

journal homepage: www.elsevier.com/locate/jcat

Impact of solvent for individual steps of phenol hydrodeoxygenation with Pd/C and HZSM-5 as catalysts

Jiayue He [a], Chen Zhao [a,*], Johannes A. Lercher [a,b,*]

[a] Department of Chemistry and Catalysis Research Center, Technische Universität München, Lichtenbergstraße 4, 85747 Garching, Germany
[b] Institute for Integrated Catalysis, Pacific Northwest National Laboratory, 902 Battelle Boulevard, Richland, WA 99352, USA

ARTICLE INFO

Article history:
Received 5 May 2013
Revised 8 September 2013
Accepted 13 September 2013

Keywords:
Phenol hydrodeoxygenation
Individual steps
In situ liquid IR spectroscopy
Kinetics
Solvent effect

ABSTRACT

Impacts of water, methanol, and hexadecane solvents on the individual steps of phenol hydrodeoxygenation are investigated over Pd/C and HZSM-5 catalyst components at 473 K in presence of H_2. Hydrodeoxygenation of phenol to cyclohexane includes four individual steps of phenol hydrogenation to cyclohexanone on Pd/C, cyclohexanone hydrogenation to cyclohexanol on Pd/C, cyclohexanol dehydration to cyclohexene on HZSM-5, and cyclohexene hydrogenation to cyclohexane on Pd/C. Individual phenol and cyclohexanone hydrogenation rates are much lower in methanol and hexadecane than in water, while rates of cyclohexanol dehydration and cyclohexene hydrogenation are similar in three solvents. The slow rate in methanol is due to the strong solvation of reactants and the adsorption of methanol on Pd, as well as to the reaction between methanol and the cyclohexanone intermediate. The low solubility of phenol and strong interaction of hexadecane with Pd lead to the slow rate in hexadecane. The apparent activation energies for hydrogenation follow the order $E_{a\ \mathrm{phenol}} > E_{a\ \mathrm{cyclohexanone}} > E_{a\ \mathrm{cyclohexene}}$, and the sequences of individual reaction rates are reverse in three solvents. The dehydration rates $\left(1.1\text{–}1.8 \times 10^3\ \mathrm{mol\ mol_{BAS}^{-1}\ h^{-1}}\right)$ and apparent activation energies (115–124 kJ $\mathrm{mol^{-1}}$) are comparable in three solvents. In situ liquid-phase IR spectroscopy shows the rates consistent with kinetics derived from chromatographic evidence in the aqueous phase and verifies that hydrogenation of phenol and cyclohexanone follows reaction orders of 1.0 and 0.55 over Pd/C, respectively. Conversion of cyclohexanol with HZSM-5 shows first-order dependence in approaching the dehydration–hydration equilibrium in the aqueous phase.

Published by Elsevier Inc.

1. Introduction

Hydrodeoxygenation is considered to be an effective approach to remove the oxygen from the products of low rank coal and oil shale, and especially of biomass liquefaction [1]. Since the oxygen content of biomass (up to 50 wt.%) markedly exceeds that of coal (below 10 wt.%), advanced catalytic approaches are required for economically feasible deoxygenation of biomass and its derivatives. Solvents dramatically influence the rates and selectivity in these catalytic processes, by changing the reactive state of these complex bio-polymers and the products in the thermal reactions. Therefore, the selection of a proper solvent is of great importance for an efficient catalytic process. However, information about the relation between solvent nature, the activity and selectivity of the catalysts, and the state of the reactant is limited in the three-phase system (gas, liquid, and solid phases) during the hydrodeoxygenation.

Recently, we reported that the hydrodeoxygenation of bio-derived phenolic components to cycloalkanes can be quantitatively achieved using metallic (Pd, Pt, and Ni) and liquid (H_3PO_4) or solid acid catalysts (Nafion, SO_4^{2-}/ZrO_2, HZSM-5, and HBEA,) at 473–523 K in water [2–7]. The reaction sequence of phenol hydrodeoxygenation with bifunctional sites of metal and acid sites in the aqueous phase is concluded to follow initial phenol hydrogenation to cylcohexanol/cyclohexanone and subsequent cyclohexanone hydrogenation to cyclohexanol catalyzed by metals, and then acid-catalyzed dehydration of cyclohexanol to cyclohexene, and final cyclohexene hydrogenation to cyclohexane [2–4]. It is, however, important to explore and compare the fundamental chemistry of hydrodeoxygenation of phenolic compounds in solvents of varying properties in order to understand, how the solvent environment modifies the solvent–catalyst, solvent–reactant, and reactant–catalyst interactions and how it might influence the catalyst itself.

* Corresponding authors at: Department of Chemistry and Catalysis Research Center, Technische Universität München, Lichtenbergstraβe 4, 85747 Garching, Germany (C. Zhao, J.A. Lercher). Tel.: +49 89 289 13540; fax: +49 89 289 13544.

E-mail addresses: chenzhao@mytum.de (C. Zhao), johannes.lercher@ch.tum.de (J.A. Lercher).

0021-9517/$ - see front matter Published by Elsevier Inc.
http://dx.doi.org/10.1016/j.jcat.2013.09.009

Water comprises typically 30 wt.% of raw bio-oil and is a suitable solvent for an upgrading process. Methanol has been successfully used for lignocellulose conversion especially for lignin liquefaction [8], and nonpolar solvents such as hexadecane and toluene have been employed for related hydrotreating of synthetic crude coal and oil shale [9,10]. The solvent for hydrodeoxygenation should, therefore, (i) be stable with respect to the process temperature, pressure, and catalyst, (ii) hold reactants and intermediates in solution; (iii) dissolve and transport H_2, and (iv) dissipate the heat of the highly exothermic reactions.

In this contribution, we report the detailed kinetics of individual steps for phenol hydrodeoxygenation with Pd/C or HZSM-5 in water, methanol, and hexadecane. The turnover frequencies (TOFs) and apparent activation energies for individual steps are explored. The relationships between the chemical nature of the solvents and the interactions at the gas–liquid–solid interfaces are investigated in order to understand the fundamental differences between the reactions occurring in media with differing properties. The solvent–catalyst, solvent–reactant, and reactant–catalyst interactions and their influence on the activity are discussed in this work as well. In situ liquid-phase IR spectroscopy is employed to monitor the concentrations of the reactants and products during individual reaction steps in water to obtain kinetic information.

2. Experimental section

2.1. Chemicals

All chemicals were provided from commercial suppliers: phenol (Sigma–Aldrich, 99% GC assay), cyclohexene (Sigma–Aldrich, 99% GC assay), cyclohexanol (Sigma–Aldrich, 99% GC assay), cyclohexanone (Sigma–Aldrich, ⩾99.5%, GC assay), ethyl acetate (Sigma–Aldrich, ⩾99.5%, GC assay), methanol (Sigma–Aldrich, ⩾99.93%, GC assay), hexadecane (Merck, >99%, GC assay), toluene (Sigma–Aldrich, ⩾99.5%, GC assay), hydrogen (Westfalen AG, 99.999 vol.%), nitrogen (Westfalen AG, 99.999 vol.%), synthetic air (Westfalen AG, 99.999 vol.%), and ultra water system (EASYpure II, Resistivity: 18.2 MΩ cm).

2.2. Catalysts

The Pd/C was obtained from Sigma–Aldrich (Sigma–Aldrich, 1 wt.% Pd), and HZSM-5 (Si/Al = 45) was supplied by Clariant AG. They were used without further treatment.

2.3. Catalyst characterization

2.3.1. Specific BET surface area and pore diameters

The surface areas and pore diameters were determined by N_2 adsorption. The N_2 adsorption was carried out at 77 K on a PMI automated BET sorptometer. Prior to the measurements, the samples were outgassed at 523 K for 20 h. The specific surface areas and micropore and mesopore distributions were calculated based on the BET and BJH models.

2.3.2. H_2 chemisorption

The Pd supported on activated carbon was first reduced at 733 K in presence of 0.1 MPa H_2 for 4 h before measurement. The reduced catalyst was activated at 733 K for 1 h in vacuum and then cooled to 313 K. The H_2 chemisorption and physisorption were subsequently measured in a pressure range from 1 kPa to 40 kPa. Then, the physisorbed H_2 was removed by outgassing the sample at the same temperature for 1 h. A second adsorption isotherm (physisorption) was measured. The concentration of chemisorbed hydrogen on the metal was determined by extrapolating the differential isotherm to zero H_2 pressure, and this value was used to calculate the dispersion of metal on supports.

2.3.3. Transmission electron microscopy (TEM)

TEM images were measured on a JEM-2010 Jeol transmission electron microscope operating at 120 kV. Prior to the measurements, catalyst was ground, suspended in ethanol, and dispersed by ultrasonic treatment. The dispersion was dropped on a copper grid-supported carbon film. The average cluster size was calculated by counting 300 Pd particles.

2.3.4. Temperature-programmed desorption (TPD)

HZSM-5 was activated in flowing He at 623 K for 1 h using a heating rate of 5 K min^{-1} from room temperature to 623 K. NH_3 was adsorbed by adding 10 vol.% to the He carrier gas (total flow 30 mL min^{-1}) at 423 K. The sample was purged with He for 2 h to remove physisorbed molecules. For TPD, the sample was heated in He at a rate of 10 K min^{-1} from 373 K to 1033 K for NH_3 desorption. The species desorbing was monitored by mass spectrometry (Balzers QME 200). For quantification, a reference material with known acid site concentration (HZSM-5 with Si/Al = 45) was used.

2.3.5. IR spectra of adsorbed pyridine

IR spectroscopy with pyridine as probe molecule was used to determine the acid site concentrations and distributions. The IR spectra were measured with a PerkinElmer 2000 spectrometer operated at a resolution of 4 cm^{-1}. The sample was activated at 723 K for 2 h in vacuum, and a background spectrum was recorded after the temperature decreased to 423 K. The activated sample was exposed to pyridine vapor (1.0×10^{-5} MPa) at 423 K for 0.5 h. After removing physisorbed pyridine by outgassing at 423 K for 0.5 h, the spectra were recorded.

2.3.6. Atomic absorption spectroscopy (AAS)

A UNICAM 939 AA-Spectrometer was used to determine the concentration of noble metals in the carbon supported catalyst. Before measurement, 20–40 mg of the sample was dissolved in a mixture of 1.0 mL of 37 wt.% hydrochloric acid and 1.0 mL of 65 wt.% nitric acid at the boiling point of the mixture.

2.4. Measurement of catalytic reactions

2.4.1. Individual steps of phenol hydrodeoxygenation with Pd/C and HZSM-5 catalysts

The hydrodeoxygenation of phenol to cyclohexane includes four steps: **Step 1**: phenol hydrogenation to cyclohexanone on Pd/C, **Step 2**: cyclohexanone hydrogenation to cyclohexanol on Pd/C, **Step 3**: cyclohexanol dehydration to cyclohexene on HZSM-5, and **Step 4**: cyclohexene hydrogenation to cyclohexane on Pd/C. Exploration of reaction rates was carried out at 473 K in three solvents (water, methanol, and hexadecane). Apparent activation energies were calculated from rates measured at 433, 453, 473, and 493 K.

The turnover frequencies (TOFs) defining initial reaction rates were expressed as per mole of converted reactant on per mole of surface Pd atom (or per mole of Brönsted acid site) per hour at conversions lower than 15% (except for the very fast cyclohexene hydrogenation) at 473 K in the presence of 4 MPa H_2. To control conversions in this range, the ratios of reactant to catalyst have been manipulated (Figs. 2, 4, 5, 7). H_2 gas was introduced to the reactor at the reaction temperature of 473 K in order to make the conversion data start from zero at $t = 0$.

2.4.1.1. Kinetics of individual steps of phenol hydrodeoxygenation in water. The reaction conditions for the TOF measurements are reported as footnotes in the corresponding figures. In a typical experiment exemplified by **Step 1** of phenol hydrogenation, phenol

(12.5 g), Pd/C (0.020 g, 1 wt.%), and H_2O (80 mL) were loaded in a Parr reactor (Series 4848, 300 mL); then, the autoclave was charged with 0.1 MPa N_2. After the temperature was increased to 473 K, P_{H2} (partial pressure for hydrogen) was charged to 4.0 MPa (ambient temperature). Then, stirring was initiated and the reaction time was recorded from that point. Reactions were conducted at 473 K with different duration times, or at 433, 453, 473, and 493 K for 0.5 h, with a stirring speed of 700 rpm. After reaction, the reactor was quenched by ice to ambient temperature, and the organic products were extracted with ethyl acetate and analyzed by GC/MS. Because two phases existed in the four individual steps in water, the kinetics data were collected from separate batches with varying reaction times. The number of surface Pd atoms is determined by H_2-chemisorption measurement. The Brønsted acid measured by IR spectroscopy of adsorbed pyridine is used to calculate the dehydration TOF. The measurements for calculation of apparent activation energy were conducted at 433, 453, 473, and 493 K with the reaction times of 0.5 h.

2.4.1.2. Kinetics of individual steps of phenol hydrodeoxygenation in methanol. For the reactions carried out in methanol, the procedures were similar to those described in water. But because reactants, intermediates, and products were all soluble in methanol, the in situ sampling was enabled and the solvent extractions are unnecessary. The detailed reaction conditions are presented as footnotes of the corresponding figures. For **Steps 1**, **2**, **3**, and **4**, the samples were collected in situ enabled by solubility in methanol and then analyzed by GC/MS.

2.4.1.3. Kinetics of individual steps of phenol hydrodeoxygenation in hexadecane. When using hexadecane as solvent, the samples were collected from separate batch modes at varying durations for **Step 1** (phenol hydrogenation on Pd/C) because the phenol reactant is insoluble in hexadecane. After reaction, the catalysts were collected by filtration, and toluene was added to the reactor to dissolve all organics. The homogeneous solution was analyzed by GC/MS. For **Steps 2**, **3**, and **4**, because reactants, intermediates, and products were all soluble in hexadecane, the in situ sampling was enabled and the solvent extractions are unnecessary. The detailed reaction conditions are presented as footnotes of the corresponding figures. The samples were collected in situ enabled by solubility in hexadecane and then analyzed by GC/MS.

2.5. In situ liquid-phase IR spectroscopy for measuring individual steps of phenol hydrodeoxygenation in water

The in situ liquid IR measurements were performed with a React IR 1000 spectrometer (Mettler Toledo) connected to an autoclave (100 mL, Parr). A diamond placed in the bottom of the autoclave was used as a probe to collect the in situ liquid IR spectra in the liquid phase. First, a background was collected with the working system containing water solvent (50 mL) and catalyst (1 wt.% Pd/C 0.10 g or HZSM-5 0.040 g) at 473 K in the presence of 4.0 MPa H_2. Second, after the reactor was cooled to ambient temperature, the individual reactions for phenol and cyclohexanone hydrogenation (**Steps 1 and 2**) were carried out at 473 K. When the temperature reached 473 K, a 4.0 MPa H_2 was introduced to the autoclave and the IR spectroscopy initiated. For dehydration of cyclohexanol (Step 3), the autoclave was charged with 1.5 MPa H_2 at ambient temperature and the IR spectrometer started. The IR spectra were collected every 10 min for 240 min during the overall reaction. Background spectra were subtracted before analysis.

3. Results and discussion

3.1. Catalyst characterizations

The physicochemical properties of 1 wt.% Pd/C and HZSM-5 catalysts are compiled in Table 1. Pd/C had a high BET surface area of 1103 $m^2\,g^{-1}$ and pore volume of 0.58 $cm^3\,g^{-1}$ with a Pd dispersion of 51% determined by H_2 chemisorption. The average Pd nanoparticle size was 2.6 nm measured by TEM (Fig. S1 in SI), agreeing reasonably well with the H_2 chemisorption result (2.2 nm). For HZSM-5, the apparent BET specific surface area was 395 $m^2\,g^{-1}$ and the pore volume was 0.26 $cm^3\,g^{-1}$ determined by N_2 sorption. The total acid concentration of HZSM-5 was 0.359 mmol g^{-1}. The Brønsted acid sites (BAS) and Lewis acid sites (LAS) were 0.278 mmol g^{-1} and 0.048 mmol g^{-1}, respectively, measured by IR spectra of adsorbed pyridine (Py-IR) (Table 1). The acid concentration determined by TPD-NH_3 was 10% higher than those analyzed by Py-IR, because the smaller size of probe molecule NH_3 allows it to reach more sterically limited acid sites comparing to pyridine.

3.2. Hydrodeoxygenation of phenol in three solvents

We have previously evaluated combinations of mono-functional catalysts with metal or acid sites for hydrodeoxygenation of phenol in water [2–6]. We now investigate the kinetics of individual steps of phenol hydrodeoxygenation with a specific combination of supported Pd and HZSM-5 in water, methanol, or hexadecane. Water has a highest polarity index 9.0 (Table 2), methanol is lower at 6.6, and hexadecane is nonpolar with the lowest polarity index of 0.3 [11]. H_2 solubility at 298 K and 0.1 MPa H_2 decreases from hexadecane (4.7×10^{-6} mol cm^{-3}) via methanol (3.5×10^{-6} mol cm^{-3}) to water (7.8×10^{-7} mol cm^{-3}) (Table 2) [12,13].

We expect the solubility of reactants, intermediates, and products to influence the reaction rates and apparent energies of activation through variations in solvent–catalyst, solvent–reactant, and reactant–catalyst interactions, as well as via potentially induced diffusion limitations. Vigorous stirring of the liquid-phase ensures the absence of external gas–liquid mass transfer diffusion limitations in this four-phase reaction, verified in the previous kinetic study in water that the individual reaction steps were not influenced by stirring speeds varied from 700 to 1000 rpm or varied reactant/water or reactant/catalyst ratios [4]. In addition, solubility of phenol, its derived intermediates, and products is different in various solvents (Table 3). Water is partially miscible with phenol, cyclohexanone, and cyclohexanol at 298 K, but cyclohexene and cyclohexane are nearly immiscible in water. Phenol, ketone, alcohol, and alkene/ane are soluble in methanol at 298 K. In

Table 1
Physicochemical properties of the selected catalysts.

Catalyst	Pd/C	HZSM-5 (Si/Al = 45)
Metal loading (wt.%)	1.0	–
BET surface area ($m^2\,g^{-1}$)	1103	395
Mesopore surface area ($m^2\,g^{-1}$)	107	173
Micropore surface area ($m^2\,g^{-1}$)	996	222
Pore volume ($cm^3\,g^{-1}$)	0.58	0.26
Mesopore volume ($cm^3\,g^{-1}$)	0.14	0.18
Micropore volume ($cm^3\,g^{-1}$)	0.44	0.08
Pd dispersion (%)	51	–
Pd particle diameter (nm) (H_2 Chemisorption)	2.2	–
Metal particle diameter (nm) (TEM)	2.6	–
Acidity (mmol g^{-1}) (TPD)	–	0.359
Acidity (mmol g^{-1}) (Py-IR)	–	BAS: 0.278 LAS: 0.048

Table 2
Solvent polarity index and H_2 solubility in three solvents (298 K and 0.1 MPa H_2) [11–13].

Solvent	Polarity	H_2 solubility (mol cm^{-3})
Water	9.0	7.8×10^{-7}
Methanol	6.6	3.5×10^{-6}
Hexadecane	ca. 0.3[a]	4.7×10^{-6}

[a] The value is estimated from the polarity index of *n*-decane (0.3), *n*-octane (0.4), and *n*-hexane (0).

hexadecane, phenol is completely insoluble, but the other intermediates and product ketone, alcohol, and alkene/ane are highly soluble at 298 K (Table 3) [14].

3.2.1. Reaction sequence of phenol hydrodeoxygenation to cyclohexane

3.2.1.1. Reaction pathways of phenol hydrodeoxygenation in water and in hexadecane. It has been established that with a combination of two mono-functional catalysts, phenol hydrodeoxygenation to cycloalkane proceeds in the aqueous phase through four steps (Scheme 1), i.e., phenol hydrogenation to cyclohexanol/cyclohexanone on metal sites (**Step 1**), sequential cyclohexanone hydrogenation to cyclohexanol on metal sites (**Step 2**), cyclohexanol dehydration to cyclohexene on acid sites (**Step 3**), and finally cyclohexene hydrogenation to cyclohexane on metal sites (**Step 4**). In hexadecane or water, the reaction pathways are identical for phenol hydrodeoxygenation with Pd/C and HZSM-5; hydrogenation is followed by dehydration (Scheme 1), but in methanol, the reaction pathway is more complex because of the acetal reactions between the cyclohexanone intermediate and methanol.

3.2.1.2. Hydrodeoxygenation pathway of phenol in methanol. The product distribution from phenol conversion in methanol is plotted in Fig. 1a as a function of time with Pd/C and HZSM-5 at 473 K. At $t = 0$, the primary product was cyclohexanone [4]. The ketone was rapidly consumed via the acetal reaction (**Route 2** in Fig. 1b) but not by the parallel hydrogenation route (**Route 1** in Fig. 1b). The selectivity to the primary acetal product (Compound **A**, methoxycyclohexanol formed from cyclohexanone and methanol, Fig. 1b) remained very low (<5 C%) during the reaction. Compound **A** was either rapidly dehydrated by HZSM-5 (**Route 3**) and hydrogenated over Pd to cyclohexyl methyl ether (Compound **B**), or this intermediate reacted further with methanol to form 1,1′-dimethoxycyclohexane (Compound **C**, **Route 2**, slower than **Route 3**) (Fig. 1b). Thus, cyclohexyl methyl ether (Compound **B**) became the major product with 81% selectivity at 170 min.

The selectivity to 1,1′-dimethoxycyclohexane (Compound **C**) first increased to a maximum of 29% at 10 min and then decreased to 3.3% at 170 min. The initial selectivity increased, because the acetal product was able to react with a large excess of methanol. The subsequent decrease in selectivity is mainly related to the fact that the increasing concentrations of water formed from the dehydration of methoxycyclohexanol (Compound A) shifted the equilibrium of 1,1′-dimethoxycyclohexane (Compound **C**) to methoxycyclohexanol (Compound **A**) (Fig. 1b), and thus, decreased the selectivity of 1,1′-dimethoxycyclohexane (Compound **C**).

With methanol as solvent, cyclohexane was produced with selectivity as low as 1.9% at 100% conversion after 170 min via **Route 1**. The fast acetal reaction between ketone and methanol (**Route 2**) dominated the phenol conversion in methanol. The acetal reaction was much faster than cyclohexanone hydrogenation on Pd/C in methanol under these reaction conditions (Fig. 1b). Thus, alcohols or polyols are not suitable solvents for hydrodeoxygenation of phenolic compounds to produce hydrocarbon biofuels, although it has been reported that lignin is efficiently converted in supercritical methanol [15].

3.2.2. Turnover frequencies (TOFs) of individual steps for phenol hydrodeoxygenation in three solvents

3.2.2.1. TOFs for phenol hydrogenation over Pd/C. In the first phenol hydrogenation step on Pd/C (**Step 1**, the first individual step), the initial TOFs in methanol $\left(1.3 \times 10^3 \text{ mol mol}^{-1}_{\text{Pd surf.}} \text{ h}^{-1}\right)$ and hexadecane $\left(7.8 \times 10^2 \text{ mol mol}^{-1}_{\text{Pd surf.}} \text{ h}^{-1}\right)$ were significantly lower than in water $\left(4.2 \times 10^3 \text{ mol mol}^{-1}_{\text{Pd surf.}} \text{ h}^{-1}\right)$ (Fig. 2, Table 4). Three factors influence the initial hydrogenation rates in methanol. The first is the solvation of phenol (solvent–reactant interaction). In the case of acetophenone conversion, Bertero et al. [16] reported that its solvation increased in the sequence 2-propanol < 1-propanol < ethanol < methanol. The opposite trend was observed for acetophenone hydrogenation rates with Ni/SiO_2, explained by the fact that stronger solvent–reactant interaction (solvation) reduced the surface coverage of the reactant. The hydrogenation rate showed 0–1 reaction order with respect to the phenol concentrations, e.g., a reaction order of 0.65 was obtained on Pd/Ca-Al_2O_3 at 503 K [17]. Thus, we hypothesize that the stronger solvation of phenol in methanol than in water or hexadecane reduces its adsorption on Pd and lowers the phenol hydrogenation rate.

The second consideration is related to the interaction of methanol with the Pd surface (solvent–catalyst interaction). Solvent adsorption on the catalyst surface may have strongly influenced the Pd activity for phenol hydrogenation. For example, methanol may compete for the catalyst surface and decrease surface coverage of phenol. Sexton et al. [18] reported that CH_3OH adsorbed more strongly than water on Pd and, thus, affects the surface phenol coverage more strongly than water.

The third impact results from the reaction between cyclohexanone and methanol (Fig. 1). The hydrogenated cyclohexanone

Table 3
Solubilities of phenol, cyclohexanone, cyclohexanol, cyclohexene, and cyclohexane at 298 K (g·(100 mL)$^{-1}$) [12].

Solvent	Phenol	Cyclohexanone	Cyclohexanol	Cyclohexene	Cyclohexane
Water	8.3	5.0	3.6	0.025	Immiscible
Methanol	>62.5	>62.5	>62.5	>62.5	30–33
Hexadecane	Insoluble	>62.5	>62.5	>62.5	>62.5

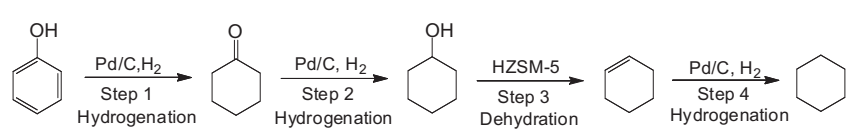

Scheme 1. Reaction sequence on hydrodeoxygenation of phenol to cyclohexane on metal and acid catalysts using water or hexadecane as solvents.

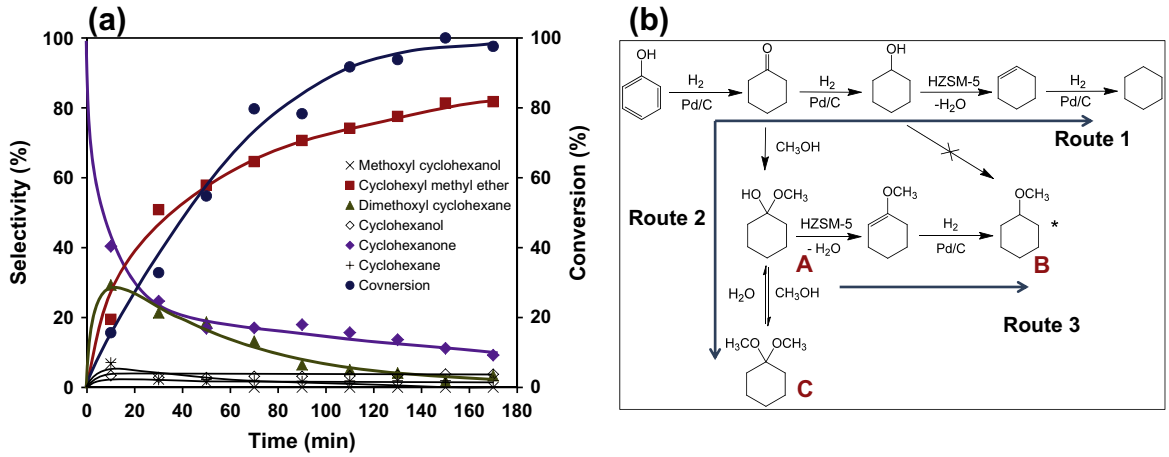

Fig. 1. (a) The product distributions during phenol hydrodeoxygenation in methanol at 473 K and 4 MPa H_2. Reaction condition: Phenol (10.0 g), CH_3OH (80 mL), Pd/C (1 wt.%, 0.20 g), HZSM-5 (Si/Al = 45, 0.02 g), stirring at 700 rpm. (b) Reaction pathways for phenol hydrodeoxygenation over Pd/C and HZSM-5 catalysts in methanol at 473 K.

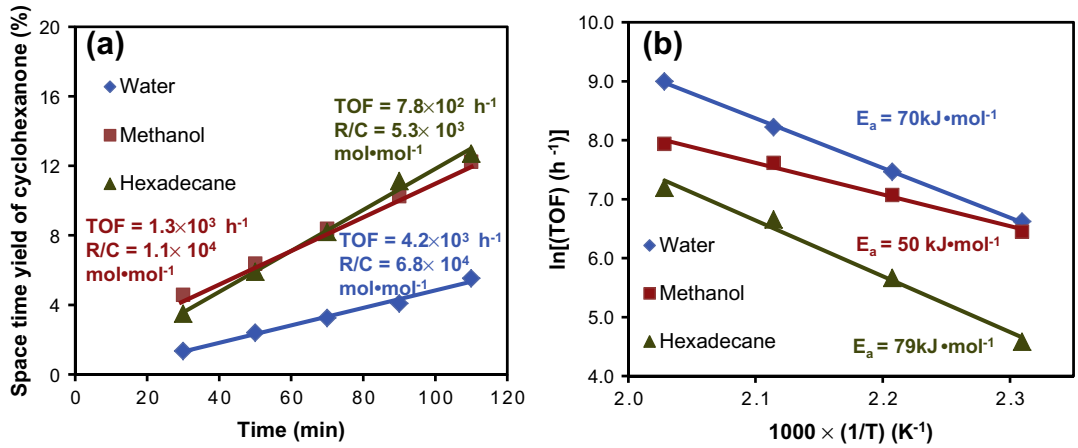

Fig. 2. (a) TOFs on phenol hydrogenation over Pd/C in three solvents at 473 K and 4 MPa H_2 at a stirring speed of 700 rpm. *Note*: R/C is mol (reactant) to mol (catalyst) ratio. Reaction conditions: phenol (12.5 g), H_2O (80 mL), and Pd/C (1 wt.%, 0.020 g); phenol (15.0 g), CH_3OH (80 mL), and Pd/C (1 wt.%, 0.15 g); phenol (5.0 g), hexadecane (80 mL), and Pd/C (1 wt.%, 0.10 g). (b) The TOF values for Arrhenius plots were recorded after 30 min at 433, 453, 473, and 493 K.

reacted quickly with methanol to form a series of products via the acetal reaction (Fig. S2 in SI). Consequently, the acetal products cyclohexyl methyl ether and dimethoxycyclohexane dominated with selectivity exceeding 85%. However, if 1,1′-dimethoxycyclohexane were preferably adsorbed on Pd sites, phenol hydrogenation would have been inhibited.

In hexadecane, the rate of phenol hydrogenation was lowered by two major factors. One is the low solubility of phenol in hexadecane (Table 3), limiting the phenol concentrations (0.26 mg L^{-1} at 298 K, detected by GC) close to the accessible Pd/C sites and inducing a diffusion limitation. The second is related to the solvent–Pd interaction, as the phenol hydrogenation rate decreased with increased strength of solvent adsorption on the Pd surface. It has been reported that the adsorption energies of hexadecane on Pd(111) and Pt(111) were ca. 118 kJ mol^{-1} [19], while in a comparative study, the adsorption energy of water on Pd(111) was 50 kJ mol^{-1} [20]. This indicates again that the hexadecane–Pd interaction is much stronger than the water–Pd interaction, which would reduce the surface concentration of phenol on Pd. In line with this argument, the hydrogenation rate in water is five times that in hexadecane.

In comparison with methanol and hexadecane, water gave the highest phenol hydrogenation rate. Phenol had low solubility in water (8.3 g·100 mL^{-1}) at ambient temperature, but the phenol solubility increased to completely miscible in water at 338 K. Thus, the solubility of phenol in water at 473 K would not limit the reaction rate. In the second consideration, the H_2 solubility in water is lower (7.8×10^{-7} mol cm^{-3}) than in hexadecane (4.7×10^{-6} mol cm^{-3}) or methanol (3.5×10^{-6} mol cm^{-3}), and the soluble H_2 concentration in water was 0.0232 mol cm^{-3} at 473 K in the presence of 4 MPa H_2 [21]. The result shows that the hydrogenation rates are more affected by the solvent properties, but not (as to be expected) by the H_2 solubility at conditions selected, which is in accordance with the previous report for hydrogenation of aromatics [22].

3.2.2.2. TOFs of cyclohexanone hydrogenation over Pd/C. Cyclohexanone reacted with methanol to form methoxycyclohexanol (Compound A) as initial product through the acetal reaction (Fig. 3a and b) and further to form 1,1-dimethoxycyclohexane (Compound C) via **Route 1** (Fig. 3b). The methoxycyclohexanol (Compound A) intermediate can also dehydrate to cyclohexenylmethyl ether catalyzed by protons in hot water (**Route 2** in Fig. 3b) and hydrogenate to cyclohexylmethyl ether (Compound B, major product at selectivity of 50% at 110 min). In a separate experiment on cyclohexanol conversion in methanol using Pd/C, the ether yield

Table 4
TOFs (h^{-1}) of hydrodeoxygenation of phenol in three solvents (473 K, 4 MPa H_2).

Solvent	Phenol hydrogenation over Pd/C TOF_1 $\left(mol\ mol^{-1}_{Pd\ surf.}\ h^{-1}\right)$	Cyclohexanone hydrogenation over Pd/C TOF_2 $\left(mol\ mol^{-1}_{Pd\ surf.}\ h^{-1}\right)$	Cyclohexanol dehydration over HZSM-5 TOF_3 $\left(mol\ mol^{-1}_{BAS}\ h^{-1}\right)$	Cyclohexene hydrogenation over Pd/C TOF_4 $\left(mol\ mol^{-1}_{Pd\ surf.}\ h^{-1}\right)$
Water	4.2×10^3	2.1×10^4	1.6×10^3	6.0×10^6
Methanol	1.3×10^3	3.5×10^3	1.8×10^3	5.6×10^6
Hexadecane	7.8×10^2	5.1×10^3	1.1×10^3	7.7×10^6

was only 0.4%, and, thus, another possible route (**Route 3**) via intermolecular dehydration forming cyclohexyl methyl ether is excluded. The kinetics of cyclohexanone conversion in methanol with Pd/C showed that conversion already attained 15% at $t = 0$ after the pre-heating process (Fig. 3a), and it is concluded that this conversion is due to the non-catalytic acetal reaction between cyclohexanol and methanol at 473 K. This is supported by the separate blank test that the cyclohexanone already reached 13% conversion after 15 min. In the first 10 min, this acetal reaction between cyclohexanone and methanol consumed 15% of the cyclohexanone. This would slow the rate for **Step 2** over Pd/C as the cyclohexanone hydrogenation rate had nearly first-order ($n = 0.8$) dependence on the reactant concentration [23]. It is estimated that with the lowered cyclohexanone concentration, the rate in methanol would be increased to 4.1×10^3 mol $mol^{-1}_{Pd\ surf.}$ h^{-1} over Pd/C, which is slightly higher than the experimental rate $\left(3.5 \times 10^3\ mol\ mol^{-1}_{Pd\ surf.}\ h^{-1}\right)$. Strong solvation of cyclohexanone and the Pd surface by methanol [18] further decreased the cyclohexanone hydrogenation rate $\left(\text{experimental result}: 3.5 \times 10^3\ mol\ mol_{Pd\ surf.}^{-1}\ h^{-1};\ \text{expected}: 4.1 \times 10^3\ mol\ mol^{-1}_{Pd\ surf.}\ h^{-1}\right)$.

In the cyclohexanone hydrogenation rate in water over Pd/C $\left(TOF = 2.1 \times 10^4\ mol\ mol^{-1}_{Pd\ surf.}\ h^{-1}\right)$ was six times that in methanol $\left(TOF = 3.5 \times 10^3\ mol\ mol^{-1}_{Pd\ surf.}\ h^{-1}\right)$ and four times that in hexadecane $\left(TOF = 5.3 \times 10^3\ mol\ mol^{-1}_{Pd\ surf.}\ h^{-1}\right)$ (Fig. 4a, Table 4). The rates of cyclohexanone hydrogenation were three to seven times those of phenol hydrogenation (Table 4), because Pd metal sites have a stronger interaction with a ketone functional group than with the aromatic ring. Since cyclohexanone did not populate Pd active sites, a lower rate of cyclohexanone hydrogenation was observed in hexadecane. This is because hexadecane has much stronger adsorption strength than water to Pd as noted previously [19,20].

3.2.2.3. TOFs for cyclohexanol dehydration over HZSM-5. The TOFs of cyclohexanol dehydration (Step 3, the third individual step) were similar at 1.1×10^3–1.8×10^3 mol mol^{-1}_{BAS} h^{-1} in water, methanol, and hexadecane, respectively (Fig. 5a and Table 4). HZSM-5-catalyzed dehydration rates in water $\left(1.6 \times 10^3\ mol\ mol^{-1}_{BAS}\ h^{-1}\right)$ were two orders of magnitude higher than H_3PO_4 did $\left(15\ mol\ mol^{-1}_{[H^+]}\ h^{-1}\right)$ [4]. The water solvent shifted the dehydration–hydration equilibrium and inhibited dehydration. It has been reported that Lewis acid sites are ineffective for dehydration in aqueous phase, because water blocks Lewis active sites [24]. Consequently, the Brønsted acid sites in the pores of zeolite are concluded to be the active catalytic sites for dehydration. We attribute the high dehydration rates on HZSM-5 to the unique properties of zeolite stabilizing a favorable transition state. High alcohol adsorption capacity even in aqueous solution [25] as well as micropore size of HZSM-5 only allows the smaller alcohol monomers to approach the zeolite BAS sites. Thus, the alcohol monomer–oligomer equilibrium is rapidly shifted toward monomers to accelerate the dehydration rate [26].

The initial activity for alcohol dehydration of HZSM-5 dropped by 60% in methanol and water after 40 min (Fig. 5a), indicating deactivation appears in the liquid phase of high concentrations of cyclohexanol (38.5–63.6 wt.%, see conditions in Fig. 5a). We also found that the color of HZSM-5 changed from white to brown, which may be caused by carbon deposition in the autoclave after reaction in water or methanol, while the color of catalyst in hexadecane was unchanged. Noller and Kladnig [27] reported that the gas-phase alcohol dehydration was accompanied by carbon deposition from the oligomerization of the formed olefins in the zeolite. Xu and Haw [28] also observed with ^{13}C MAS NMR oligomerized cyclohexene from cyclohexanol on HZSM-5. In fact, more carbon was deposited from the concentrated cyclohexanol liquid phase (38.5–63.6 wt.%) than from the gas phase after considering the different densities of the two phases. The decreased catalytic activities in water and methanol are mainly due to the carbon deposition formation on the catalytic material.

The catalyst, however, did not deactivate in hexadecane, and this may be attributed to the different stabilities of carbenium ions (from cyclohexanol) in the three solvents. The counter ion and the carbenium ion may have a range of associations, from a covalent bond, tight ion pair (un-separated), to solvent-separated ion pair (partially separated) and free ions (completely dissociated) (Scheme 2) [29,30]. The covalent bond association is strongest and the association of free ions is weakest [30]. In cationic polymerization, the ions are in equilibrium between an associated ion pair and free ions [29]. Ion pair separation is favored by more polar solvents. Since free ions are more reactive than ion pairs, the rate of propagation is faster in more polar solvents. Therefore, polar water (polarity index: 9.0) and methanol (polarity index: 6.6) yield higher polymerization selectivity than hexadecane (polarity index: 0.3).

The intermolecular dehydration of cyclohexanol in water formed bicyclohexyl ether with 10% selectivity at 110 min. Cyclohexanol reacted with methanol via intermolecular reaction as well. Shown from the kinetics of cyclohexanol dehydration (Fig. 6a), the parallel routes of intra-molecular dehydration producing cyclohexene and of intermolecular dehydration forming cyclohexyl methyl ether maintained individual selectivities of 75% and 25% during the conversion (Fig. 6b), respectively.

3.2.2.4. TOFs for cyclohexene hydrogenation over Pd/C. Cyclohexene hydrogenation rates (Step 4, the fourth individual step) were similar in these three solvents at attaining TOFs of 5.6×10^6–7.7×10^6 mol $mol^{-1}_{Pd\ surf.}$ h^{-1} (Fig. 7, Table 4). This is in line with results obtained by Gonzo and Boudart [31], who also reported the absence of a solvent effect for hydrogenation of cyclohexene on Pd/SiO_2 after studying the influence of diverse solvents of methanol, *n*-heptane, ethyl acetate, and cyclohexane at 308 K.

Combining all the data obtained from kinetics of the four individual reactions distinguishes the rate-determining step for the phenol hydrodeoxygenation in the three solvents (Table 4). In water, cyclohexanol dehydration (**Step 3**) was the slowest step. The rate-determining step in methanol and hexadecane was

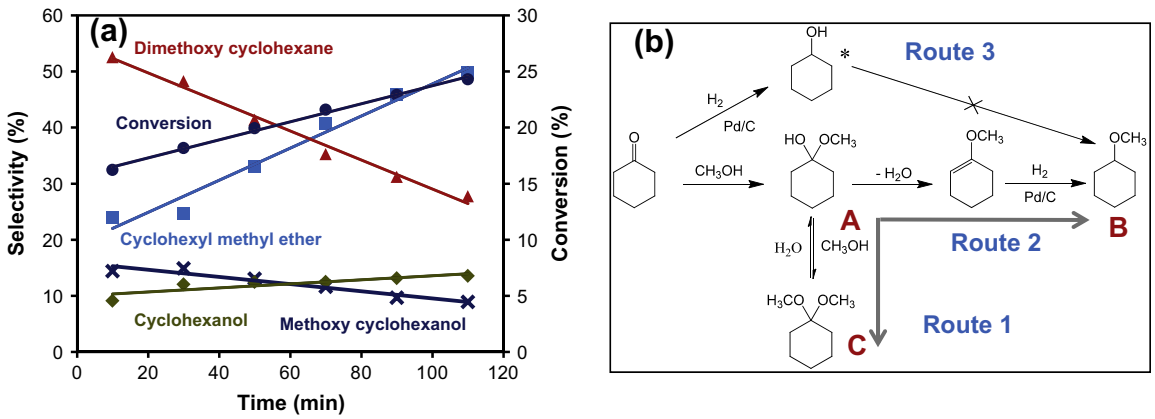

Fig. 3. (a) The conversion/selectivity of cyclohexanone hydrogenation in methanol at 473 K and 4 MPa H_2 at a stirring speed of 700 rpm. Reaction condition: cyclohexanone (20.0 g), CH_3OH (80 mL), and Pd/C (1 wt.%, 0.010 g). (b) Reaction pathways for cyclohexanone hydrogenation over Pd/C in methanol.

phenol hydrogenation (**Step 1**). Based on these results, it is expected that in the use of dual-functional catalysts of Pd/C and HZSM-5 for phenol hydrodeoxygenation in water, if not considering the competitive adsorption of the reactants in the overall kinetics, the most abundant product is cyclohexanol as dehydration (**Step 3**) is relatively slow compared to hydrogenation. When phenol starts to be hydrogenated on Pd/C (**Step 1**) in hexadecane, cyclohexane is expected to appear as the major product in a short time, because the rates of cyclohexanone hydrogenation (**Step 2**), via cyclohexanol dehydration (**Step 3**), to cyclohexene hydrogenation (**Step 4**) are accelerated step by step. Rates of cyclohexanol dehydration and cyclohexene hydrogenation were similar in three solvents, but the rates of hydrogenation of phenol and cyclohexanone were much slower in methanol and hexadecane compared to the rates in water.

3.2.3. E_a of the individual steps in phenol hydrodeoxygenation

The individual steps during phenol hydrodeoxygenation can be grouped into (i) hydrogenations of aromatic ring, ketone, and alkene on Pd and (ii) dehydration of cyclohexanol on HZSM-5. For the three hydrogenation steps, it was found that the apparent activation energies for hydrogenation were similar in hexadecane and water, but significantly lower in methanol (Table 5).

The observed activation energy equation can be expressed as follows[32]:

$$E_a^{obs} = E_a^{true} + (1 - \theta_A)\ \Delta H_A - \theta_B \Delta H_B \quad (1)$$

where E_a^{obs}, E_a^{true} θ_A, θ_B, ΔH_A, and ΔH_B represent the observed activation energy, the true activation energy, the coverage by reactant, the coverage by product, the reactant heat of adsorption, and the product heat of adsorption, respectively.

The phenol hydrogenation rates were recorded in three solvents at 433, 453, 473, and 493 K. Based on the Arrhenius law, the activation energies (E_a) were calculated to be 70, 50, and 79 kJ mol^{-1} in water, methanol, and hexadecane, respectively. Vishwanathan and Mahata [33] obtained an apparent activation energy of 65 kJ mol^{-1} for phenol hydrogenation over Pd/MgO in the gas phase in fair agreement of our result (Table 5). By comparison, E_a for the phenol hydrogenation in hexadecane was similar to that in water at 70–79 kJ mol^{-1}. E_a in methanol was significantly lower at 50 kJ mol^{-1} (Table 5). We attribute this to the strong solvation of both phenol [16] and surface Pd [18] by methanol. Solvation would lower the θ_A and θ_B in Eq. (1). Consequently, E_a^{obs} in methanol would be lower than in water or hexadecane. Moreover, the reaction with methanol of the cyclohexanone generated from phenol hydrogenation would also decrease θ_A and θ_B because of competing by-product adsorption, and thus lower E_a^{obs} in methanol.

The E_a of cyclohexanone hydrogenation followed the same trend as phenol hydrogenation; hexadecane (48 kJ mol^{-1}) > water (37 kJ mol^{-1}) > methanol (28 kJ mol^{-1}). E_a for the hydrogenation

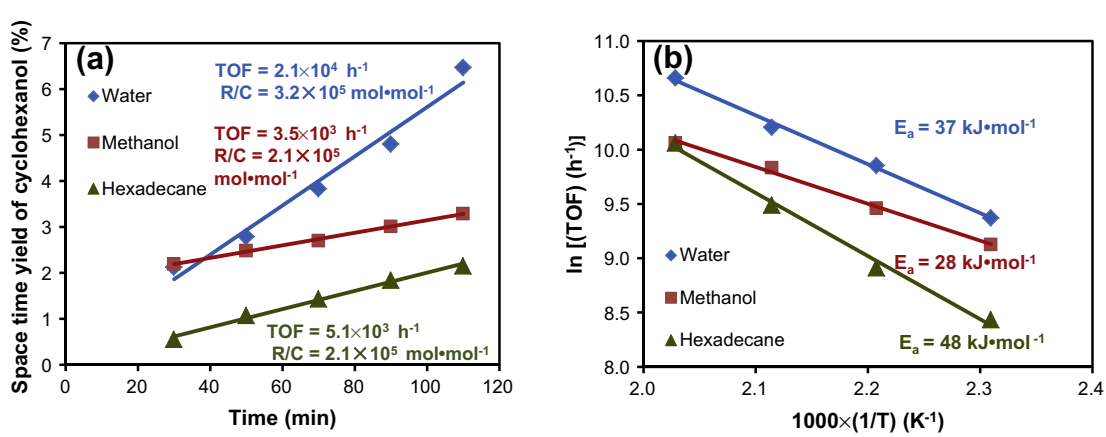

Fig. 4. (a) TOFs of cyclohexanone hydrogenation over Pd/C in three solvents at 473 K and 4 MPa H_2 at a stirring speed of 700 rpm. *Note*: R/C stands for mol (reactant) to mol (catalyst). Reaction conditions: cyclohexanone (60.0 g), H_2O (80 mL), and Pd/C (1 wt.%, 0.020 g); cyclohexanone (20.0 g), CH_3OH (80 mL), and Pd/C (1 wt.%, 0.010 g); cyclohexanone (20.0 g), hexadecane (80 mL), and Pd/C (1 wt.%, 0.010 g). (b) The TOF values for Arrhenius plots are recorded after 30 min at 433, 453, 473, and 493 K.

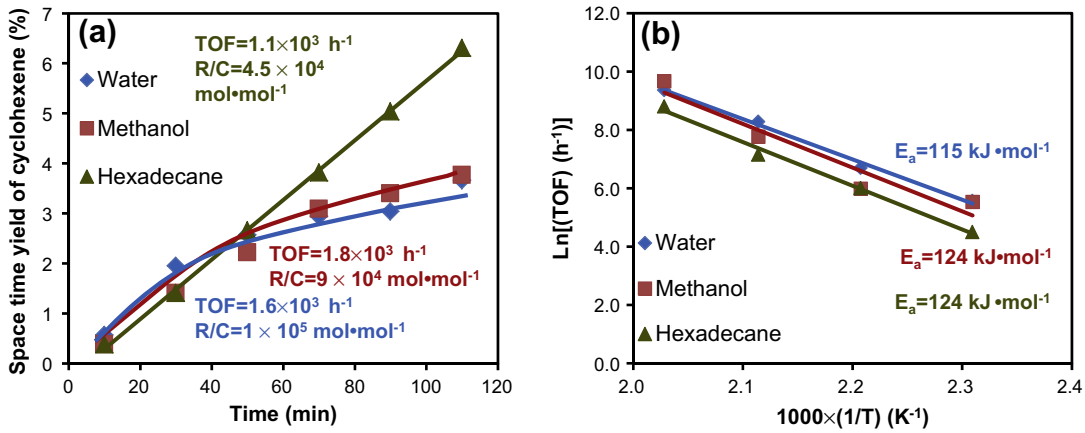

Fig. 5. (a) TOFs of cyclohexanol dehydration in three solvents at 473 K in presence of 4 MPa H_2 at a stirring speed of 700 rpm. R/C stands for mol (reactant) to mol (catalyst). Reaction conditions: cyclohexanol (140.0 g), H_2O (80 mL), HZSM-5 (0.050 g); cyclohexanol (50.0 g), CH_3OH (80 mL), HZSM-5 (0.020 g); cyclohexanol (50.0 g), hexadecane (80 mL), HZSM-5 (0.040 g). (b) The TOF values for Arrhenius plots are recorded after 3 min at 433, 453, 473, and 493 K.

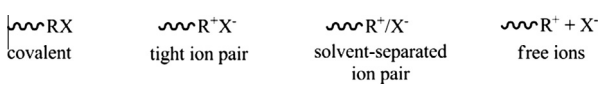

Scheme 2. Range of associations between the carbenium ion (R^+) and anion (X^-).

reaction in methanol was significantly lower than that in water or hexadecane (Table 5). Due to the similar hydrogenation mechanisms, the strong solvation of cyclohexanone by methanol [16] (Table 3) and the stronger adsorption of methanol on Pd [18] decreased the θ_A and θ_B, and resultantly lowered the apparent activation energy.

The E_a values for cyclohexanol dehydration were 115, 124, and 124 kJ mol^{-1} with HZSM-5 in water, methanol, and hexadecane, respectively. Knözinger et al. [34] measured E_a for cyclohexanol dehydration (110 kJ mol^{-1}) over γ-Al_2O_3 in a continuous flow reactor at low conversion (<10%). In our preliminary work, E_a for H_3PO_4-catalyzed cyclohexanol dehydration was calculated to be 120 kJ mol^{-1}. In the present study (Table 5), E_a for HZSM-5-catalyzed cyclohexanol dehydration in water (115 kJ mol^{-1}) was similar to that in hexadecane (124 kJ mol^{-1}) and in methanol (124 kJ mol^{-1}) and to Ni/ZSM-5-catalyzed cyclohexanol dehydration (E_a: 112 kJ mol^{-1}) in our works [35,36].

In the cyclohexene hydrogenation, E_a in water (25 kJ mol^{-1}) and in hexadecane (24 kJ mol^{-1}) were almost the same. E_a in methanol was only 12 kJ mol^{-1}. The E_a of cyclohexene hydrogenation was 32 kJ mol^{-1} in the liquid phase over Pd/SiO_2 reported by Gonzo and Boudart [31], which was a bit higher than our result. The adduct formation from methanol and cyclohexene [37] may lead to a much lower apparent E_{a4} in methanol.

Summarizing the three hydrogenation reactions in the sequence at 473 K, the activation energies decreased in the order $E_{a\ \text{phenol hydrogenation}} > E_{a\ \text{cyclohexanone hydrogenation}} > E_{a\ \text{cyclohexene hydrogenation}}$, while the reaction rates rose in the reverse sequence $TOF_{\text{phenol hydrogenation}} < TOF_{\text{cyclohexanone hydrogenation}} < TOF_{\text{cyclohexene hydrogenation}}$. It also shows that the three hydrogenation reaction apparent activation energies were much lower in methanol than in water or hexadecane, apparently due to the solvent effect including methanol–phenol and methanol–Pd interactions. The interactions of methanol with phenol, cyclohexanone, or cyclohexene altered the occupancy of Pd sites by decreasing the reactant coverage and thus also lower the apparent activation energies eventually. The rates and activation energies for dehydration catalyzed by HZSM-5 were similar in the three solvents, indicating that they led to similar interactions with reactant–HZSM-5 and product–HZSM-5.

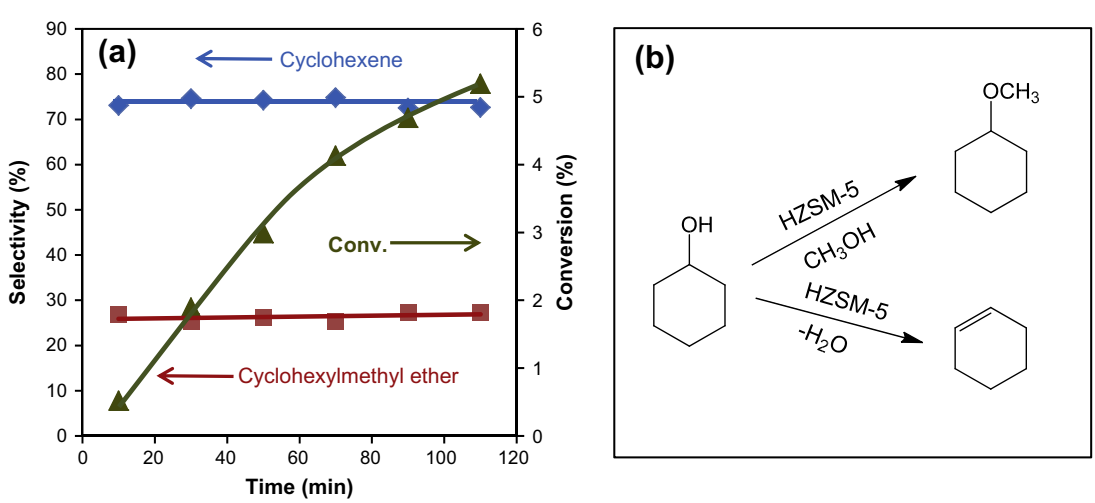

Fig. 6. (a) The product distribution from cyclohexanol dehydration in methanol at 473 K in presence of 4 MPa H_2. Reaction condition: cyclohexanol (50.0 g), CH_3OH (80 mL), HZSM-5 (Si/Al = 45, 0.020 g). (b) Reaction route for cyclohexanol dehydration over HZSM-5 in methanol.

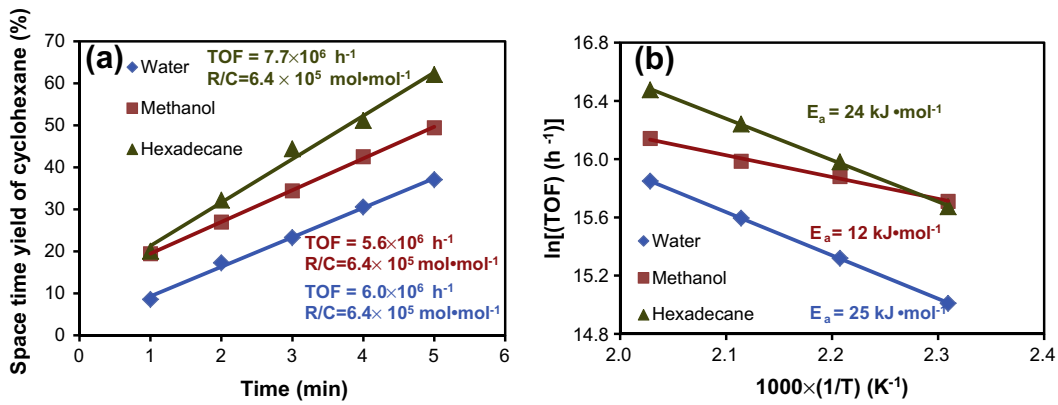

Fig. 7. (a) TOFs of cyclohexene hydrogenation over Pd/C in water, methanol and hexadecane at 473 K in 4 MPa H_2 at a stirring speed of 700 rpm. *Note*: R/C stands for mol (reactant) to mol (catalyst). Reaction conditions: cyclohexene (50.0 g), H_2O (80 mL), Pd/C (1 wt.%, 0.010 g); cyclohexene (50.0 g), CH_3OH (80 mL), Pd/C (1 wt.%, 0.010 g); cyclohexene (50.0 g), hexadecane (80 mL), Pd/C (1 wt.%, 0.010 g). (b) The TOF values for Arrhenius plots were recorded after 3 min at 433, 453, 473, and 493 K.

Table 5
E_a (kJ mol^{-1}) on hydrodeoxygenation of phenol in three solvents (473 K, 4 MPa H_2).

Solvent	Phenol hydrogenation over Pd/C E_{a1}	Cyclohexanone hydrogenation over Pd/C E_{a2}	Cyclohexanol dehydration over HZSM-5 E_{a3}	Cyclohexene hydrogenation over Pd/C E_{a4}
Water	70	37	115	25
Methanol	50	28	124	12
Hexadecane	79	48	124	24

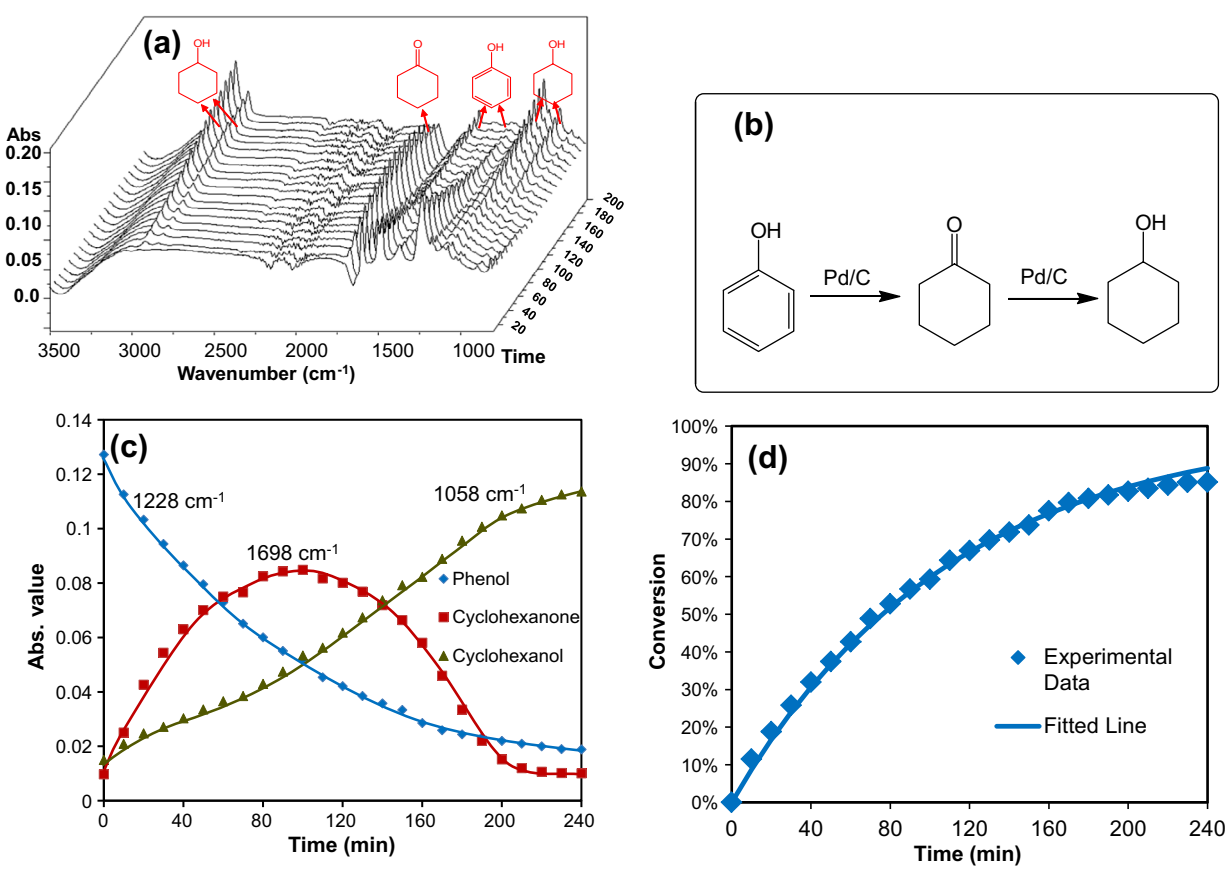

Fig. 8. (a) In situ liquid IR spectra for aqueous-phase phenol hydrogenation. Reaction conditions: phenol (10.0 g), H_2O (50.0 mL), 1 wt.% Pd/C (0.10 g), 4 MPa H_2, 473 K, stirred at 700 rpm. The spectra were collected every 10 min for 240 min. (b) Reaction pathway for phenol conversion on Pd/C in the aqueous phase. (c) IR absorbance as a function of reaction time. (d) Fitted line and experimental conversion data as a function of time based on the assumption of first-order dependence to phenol concentrations.

Table 6
Kinetic data for individual steps of phenol hydrodeoxygenation in the aqueous phase determined by in situ liquid IR and GC measurements (Normalized to the conditions in the in situ liquid IR experiments).

Kinetic data	Reactions			
	Phenol hydrogenation	Cyclohexanone hydrogenation	Cyclohexanol dehydration	Cyclohexene hydrogenation
In situ liquid IR TOF	5.0×10^3 mol $mol_{Pd\ surf^{-1}}$. h^{-1}	1.8×10^4 mol $mol_{Pd\ surf^{-1}}$. h^{-1}	2.2×10^3 mol mol_{BAS}^{-1} h^{-1}	–
Reaction order	$n_{(Phenol)}$: 1	$n_{(Cyclohexanone)}$: 0.55	$n_{(Cyclohexanol)}$: 1	–
Rate constant	9.1×10^{-3} min^{-1}	4.6×10^{-2} $mol^{0.45}$ $L^{-0.45}$ min^{-1}	1.1×10^{-2} min^{-1} [a]	–
GC TOF	4.2×10^3 mol $mol_{Pd\ surf^{-1}}$. h^{-1}	2.1×10^4 mol $mol_{Pd\ surf^{-1}}$. h^{-1}	1.6×10^3 mol_{BAS}^{-1} h^{-1}	6.0×10^6 mol $mol_{Pd\ surf^{-1}}$. h^{-1}
Reaction order	$n_{(Phenol)}$: 1	$n_{(Cyclohexanone)}$: 0.55	$n_{(Cyclohexanol)}$: 1	$n_{(Cyclohexene)}$: 0
Rate constant	3.3×10^{-3} min^{-1}	4.5×10^{-2} $mol^{0.45}$ $L^{-0.45}$ min^{-1}	7.5×10^{-3} min^{-1} [b]	5.0×10^{-2} mol L^{-1} min^{-1}

[a] The value represents the sum of $k_{dehydration}$ and $k_{hydration}$ in the aqueous phase.
[b] The value represents the $k_{dehydration}$ in the aqueous and organic phases.

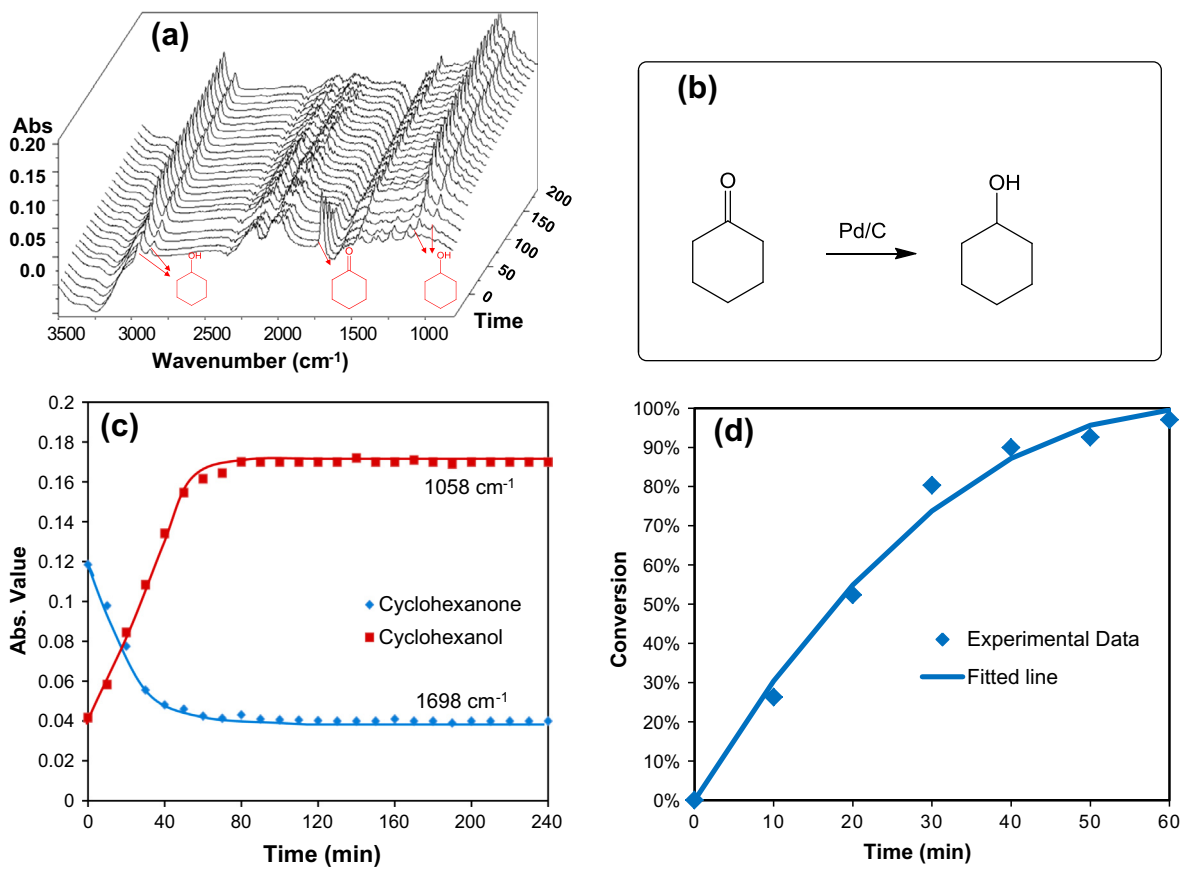

Fig. 9. (a) In situ liquid IR spectra during aqueous-phase cyclohexanone hydrogenation. Reaction conditions: cyclohexanone (10.0 g), H_2O (50.0 mL), 1 wt.% Pd/C (0.10 g), 4 MPa H_2, 473 K, stirred at 700 rpm. The spectra were collected every 10 min for 240 min. (b) Reaction pathway for cyclohexanone conversion on Pd/C in the aqueous phase. (c) IR absorbance as a function of reaction time. (d) Fitted line and experimental conversion data as a function of time based on the assumption that the order dependence to cyclohexanone concentrations is 0.55.

3.3. In situ liquid-phase IR spectroscopy for measuring the individual steps in aqueous-phase phenol hydrodeoxygenation

In order to detect the intermediates and products formed in situ during phenol conversion, and to estimate and compare the rates of individual steps, variations in concentrations of compounds are monitored by attenuated total reflectance (ATR) IR spectroscopy using diamond as a probe window for phenol hydrogenation, cyclohexanone hydrogenation, and cyclohexanol dehydration reactions in the aqueous phase. The standard IR reference spectra of water solvent with reactant, intermediates, and products are displayed in Fig. S3. The IR signals of cyclohexene hydrogenation are not observable in the aqueous phase, because cyclohexene and cyclohexane are immiscible in water (Table 3). With the IR diamond probe on the reactor floor, three individual reactions (**Steps 1**, **2**, and **3**) were carried out in the aqueous phase at 473 K and 4.0 MPa H_2.

During phenol hydrogenation over Pd/C, the intensity of the characteristic IR peak of phenol at 1228 cm^{-1} steadily decreased throughout the run shown in Fig. 8a. The intensity of the peak characteristic of cyclohexanone (partial hydrogenated from phenol) at 1698 cm^{-1} initially increased from 0 to 0.085 at 100 min and then decreased from 0.085 to 0 at extended time up to 240 min. The intensity of the characteristic peak of cyclohexanol at 1058 cm^{-1} increased very slowly in the initial 100 min, because cyclohexanol was formed by direct hydrogenation from phenol in

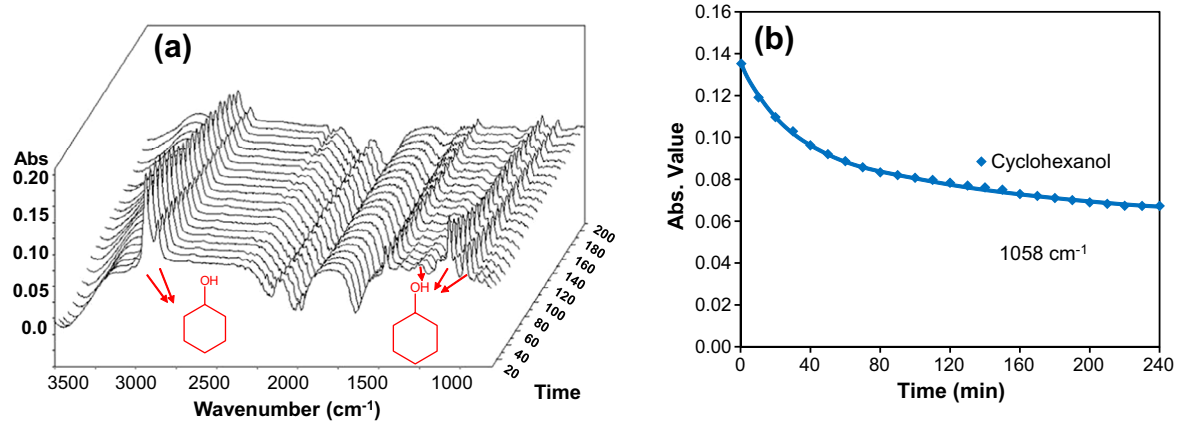

Fig. 10. (a) In situ liquid IR spectra during aqueous-phase cyclohexanol dehydration. Reaction conditions: cyclohexanol (10.0 g), H_2O (50.0 mL), HZSM-5 (0.040 g), 4 MPa H_2, 473 K, stirred at 700 rpm. The spectra were collected every 10 min for 240 min. (b) IR absorbance versus reaction time.

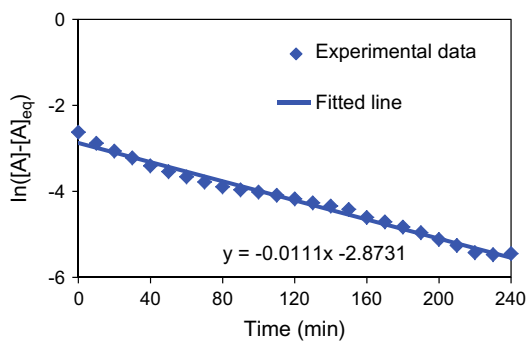

Fig. 11. Estimation the validity of a first-order reaction rate hypothesis for the cyclohexanol dehydration via ln([Cyclohexanol]–[Cyclohexanol]$_{eq}$) versus time.

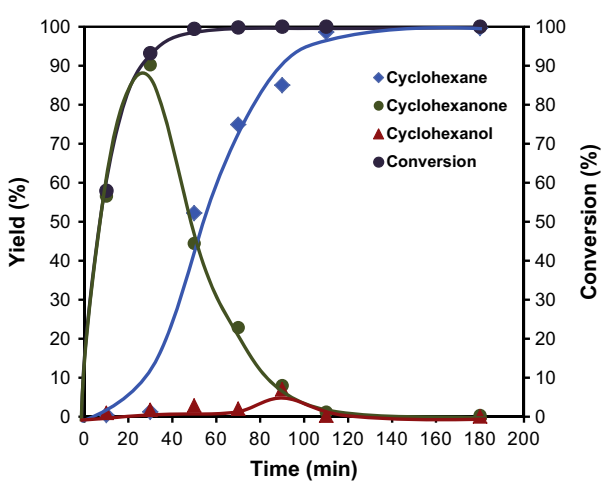

Fig. 12. The product distributions during phenol hydrodeoxygenation in the aqueous phase in the presence of Pd/C and HZSM-5. Reaction conditions: Phenol (1.0 g), 1 wt.% PdC (0.040 g), HZSM-5 (0.20 g), H_2O (80 mL), 473 K, 4 MPa H_2, stirring at 700 rpm.

the beginning. Then, the intensity rose more steeply from 100 to 240 min, as both phenol and cyclohexanone were converted to cyclohexanol at this time interval. This interesting kinetic performance is consistent with step-wise hydrogenation of phenol to cyclohexanone and subsequent hydrogenation to cyclohexanol (Fig. 8b). From the plotted data of IR absorbance versus reaction time (Fig. 8c), it can be calculated that the phenol hydrogenation rate was 5.0×10^3 mol $mol^{-1}_{Pd\ surf.}$ h^{-1}, which is similar to that obtained value from the above kinetic measurement detected by GC $\left(4.2 \times 10^3 \text{ mol mol}^{-1}_{Pd\ surf.} \text{ h}^{-1}\right)$. In addition, if assuming that it was first-order to phenol concentration, the fitted curve can be perfectly matched with the experimental data with a rate constant of 9.1×10^{-3} min^{-1} (Fig. 8d and Table 6).

In the conversion of cyclohexanone hydrogenation over Pd/C (Fig. 9a), the intensity of the characteristic IR absorbance of cyclohexanone reactant at 1698 cm^{-1} decreased rapidly and vanished at 60 min, while the intensity of characteristic IR absorbance of cyclohexanol at 1058 cm^{-1} increased quickly accordingly. The fast loss of cyclohexanone is agreement with the high cyclohexanone hydrogenation TOF. The rate of cyclohexanone hydrogenation was shown to be much faster than phenol hydrogenation through the comparison of two in situ liquid IR spectra (Figs. 8a and 9a). The cyclohexanone hydrogenation rate was 1.8×10^4 mol $mol^{-1}_{Pd\ surf.}$ h^{-1} calculated from the plots of IR absorbance versus reaction time (Fig. 9c), consistent with the value 2.1×10^4 mol $mol^{-1}_{Pd\ surf.}$ h^{-1} monitored by GC. As shown in Fig. 9d, the cyclohexanone hydrogenation rate showed the order dependence to cyclohexanone concentrations of 0.55, attaining the rate constant of 4.6×10^{-2} $mol^{0.45}$ $L^{-0.45}$ min^{-1}.

In a sequence of IR spectra taken during cyclohexanol dehydration in water over HZSM-5 (Fig. 10a), only the characteristic IR band of cyclohexanol varied, because the cyclohexene floated on the aqueous phase and was not detected by the IR detector in the bottom of the autoclave. The intensity of the cyclohexanol absorbance at 1058 cm^{-1} decreased more slowly than the former two individual reactions, in accordance with the kinetic measurement that dehydration is the rate-determining step in aqueous-phase phenol hydrodeoxygenation. Determined from the IR absorbance versus reaction time (Fig. 10b), the cyclohexanol dehydration rate was 2.2×10^3 mol mol^{-1}_{BAS} h^{-1}, agreeing with the rate of 1.6×10^3mol $mol^{-1}_{BAS}h^{-1}$ derived from chromatographic evidence.

The dehydration–hydration reaction of cyclohexanol is equilibrated over HZSM-5 in the aqueous phase as Eq. (2):

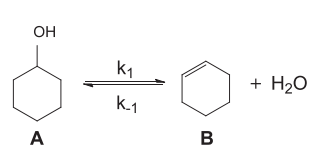

(2)

For the first-order reversible reaction with excess water:

$$-\frac{d[A]}{dt} = k_1[A] - k_{-1}[B] \quad (3)$$

$$[B] = [B]_0 + ([A]_0 - [A]) \quad (4)$$

$$\text{So } -\frac{d[A]}{dt} = k_1[A] - k_{-1}([B]_0 + ([A]_0 - [A])) \quad (5)$$

$$\text{At equilibrium, } -\frac{d[A]}{dt} = 0 \text{ and } [A]_{eq} = \frac{k_{-1}}{k_1 + k_{-1}}([B]_0 + [A]_0) \quad (6)$$

$$-\frac{d([A] - [A]_{eq})}{dt} = -\frac{d[A]}{dt} = (k_1 + k_{-1})([A] - [A]_{eq}) \quad (7)$$

$$[A] - [A]_{eq} = ([A]_0 - [A]_{eq})e^{-(k_1+k_{-1})t} \quad (8)$$

$$t = \frac{\ln([A] - [A]_{eq})}{-(k_1 + k_{-1})} + \frac{\ln([A]_0 - [A]_{eq})}{(k_1 + k_{-1})} \quad (9)$$

As shown in Fig. 11, cyclohexanol dehydration was determined to be a first-order reaction with HZSM-5 at 473 K in the aqueous phase, and $k_1 + k_{-1}$ equaled to 1.1×10^{-2} min^{-1}.

The rate constants, reaction orders, and TOFs of three individual steps in the aqueous phase, as determined by GC and in situ liquid IR detectors, are compiled in Table 6. The reaction orders in the aqueous solution have been identified by in situ liquid IR spectroscopy, that is, phenol and cyclohexanone hydrogenation over Pd/C followed reaction orders of 1.0 and 0.55, respectively. Conversion of cyclohexanol with HZSM-5 shows first-order dependence in the dehydration–hydration equilibrium. The TOFs of three aqueous-phase individual steps determined from GC measurement were very close to the values from in situ liquid IR, with minor differences of 10–20%. As shown in Table 6, the rate constants for phenol and cyclohexanone hydrogenation were comparable. Phenol hydrogenation attained a rate constant of 9.1×10^{-3} and 3.3×10^{-3} min^{-1} as measured by in situ liquid IR spectroscopy and GC, respectively, while cyclohexanone hydrogenation showed a rate constant of 4.6×10^{-2} and 4.5×10^{-2} mol$^{0.45}$ L$^{-0.45}$ min^{-1} from these two techniques. It is notable that the dehydration rate constants were quite different from two approaches, because in situ liquid-phase IR spectroscopy estimates the sum of $k_{dehydration}$ and $k_{hydration}$ (1.1×10^{-2} min^{-1}) in the aqueous phase, while the GC analysis determines $k_{dehydration}$ (7.5×10^{-3} min^{-1}) in the sum of aqueous and organic phases. The rate constant for cyclohexene hydrogenation was calculated to be 5.0×10^{-2} mol L^{-1} min^{-1} from GC measurement, as the reaction order toward cyclohexene concentration is assumed to be 0 [31].

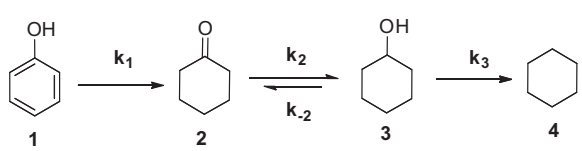

Scheme 3. Proposed elementary reaction steps in the overall phenol hydrodeoxygenation.

In a comparative study, we also performed the overall phenol hydrodeoxygenation with dual Pd/C and HZSM-5 components in the aqueous phase in order to demonstrate the cooperative effect of acid and metal sites (Fig. 12). Phenol was quantitatively converted to cyclohexane at 473 K and 4 MPa H_2 along the reaction routes discussed above. Due to the fast hydrogenation of cyclohexene intermediate on Pd/C, it was not observed in the presence of the catalyst mixture. This result agrees well with our previous studies on hydrodeoxygenation of phenol monomers and dimers as well as bio-oil with bifunctional catalysts consisting of Pd and acids [4–6]. The elementary steps in the overall phenol hydrodeoxygenation include phenol hydrogenation to produce cyclohexanone (k_1), subsequently cyclohexanone hydrogenation to afford cyclohexanol (k_2) which is in an equilibrium with cyclohexanol dehydrogenation to cyclohexanone (k_{-2}), in turn cyclohexanol is dehydrated and hydrogenated to cyclohexane (k_3) (Scheme 3).

For hydrogenation of phenol and cyclohexanone over Pd/C with varying hydrogen pressures of 3, 4, and 5 MPa, the reaction orders of hydrogen concentration for phenol and cyclohexanone hydrogenation were determined to be 1.5 and 0.6, respectively (see Figs. 13 and 14). It was observed that the hydrogen pressure before and after reaction kept unchanged; thus, the hydrogen pressures were considered as constant values in the elementary rate equations.

It is assumed first-order reaction to phenol, cyclohexanone, and cyclohexanol concentrations and zero-order reaction to cyclohexene concentration. Therefore, the overall phenol hydrodeoxygenation includes the following elementary rate equations:

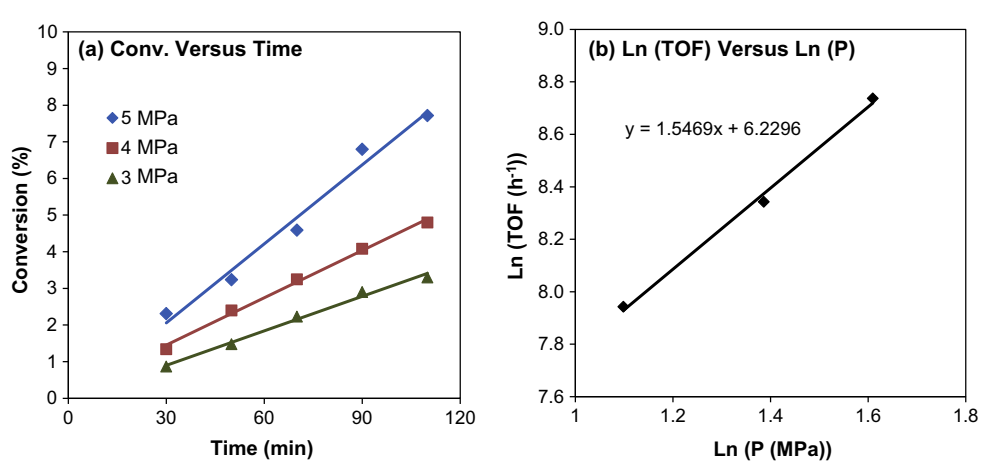

Fig. 13. Hydrogenation of phenol over Pd/C with varying hydrogen pressures. Reaction conditions: phenol (12.5 g), H_2O (80 mL), 1 wt.% Pd/C (0.02 g), 473 K, stirring at 700 rpm.

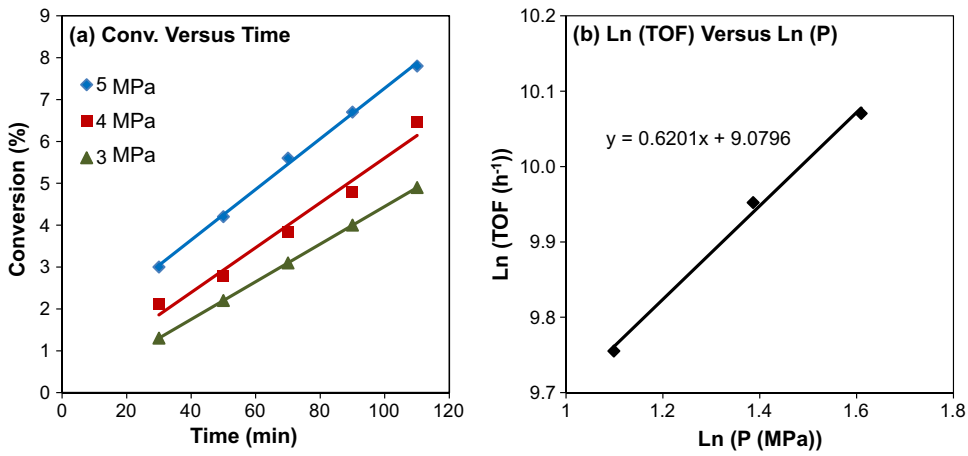

Fig. 14. Hydrogenation of cyclohexanone over Pd/C with varying hydrogen pressures. Reaction conditions: cyclohexanone (60.0 g), H_2O (80 mL), 1 wt.% Pd/C (0.02 g), 473 K, stirring at 700 rpm.

Table 7
Comparison of fitted rate constants in the overall phenol hydrodeoxygenation and in the individual steps analyzed by GC measurements (conditions: 1.0 g phenol, 0.04 g Pd/C, 0.20 g HZSM-5, 473 K, 4 MPa H_2).

Reaction rate constants	k_1 (min^{-1})	k_2 (min^{-1})	k_{-2} (min^{-1})	k_3 (min^{-1})	Fitness parameter
Fitted elementary steps in the overall HDO	9.0×10^{-2}	3.0×10^{-1}	5.4	4.0×10^{-1}	0.46
Data from individual steps analyzed by GC[a]	1.4×10^{-2}	1.8×10^{-1}	n.d.	3.8×10^{-1}	–

[a] Normalized to the conditions in the overall phenol hydrodeoxygenation experiment.

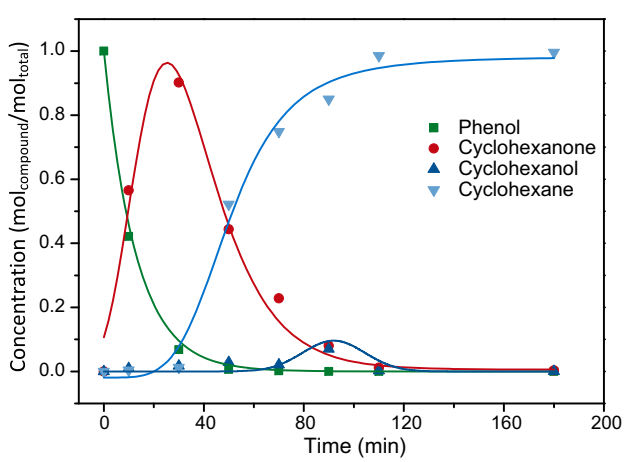

Fig. 15. Fitting the experimental data of phenol hydrodeoxygenation with Pd/C and HZSM-5 catalysts in presence of hydrogen, solid points: experiment data, line: fitted curve. Conditions: phenol (1.0 g), 1 wt.% Pd/C (0.04 g), HZSM-5 (0.20 g), 473 K, 4 MPa H_2.

$$\frac{dc_1}{dt} = -k_1 \times c_1 \tag{10}$$

$$\frac{dc_2}{dt} = k_1 \times c_1 - k_2 \times c_2 + k_{-2} \times c_2 \tag{11}$$

$$\frac{dc_3}{dt} = k_2 \times c_2 - k_{-2} \times c_2 - k_3 \times c_3 \times c(H^+) \tag{12}$$

$$\frac{dc_4}{dt} = k_3 \times c_3 \times c(H^+) \tag{13}$$

Fitting the pseudo-rate constants of the individual steps of phenol hydrodeoxygenation (Table 7 and Fig. 15), the fitted phenol hydrogenation rate constant (9.0×10^{-2} min^{-1}) was much higher than the value (1.4×10^{-2} min^{-1}) deduced as the first step in individual measurements, probably due to the added acid effect for accelerating hydrogenation rates in the overall phenol hydrodeoxygenation. But fitted apparent rate constants (3.0×10^{-1} min^{-1}) in the subsequent cyclohexanone hydrogenation elementary steps varied from that determined in individual steps (1.8×10^{-1} min^{-1}) (Table 7) due to strong competitive adsorption of phenol and cyclohexanone onto active sites during the overall phenol hydrodeoxygenation. The fitted cyclohexanol dehydration rate constant (4.0×10^{-1} min^{-1}) was slightly higher than the value (3.8×10^{-1} min^{-1}) analyzed by the individual measurement, because the dehydration–hydration equilibrium is shifted by the subsequent cyclohexene hydrogenation over combined Pd/C and HZSM-5 catalysts.

4. Conclusion

Solvents influence the rates of catalytic phenol hydrodeoxygenation by altering the H_2 solubility and the solvent–reactant interactions, as well as by competitive solvent/reactant adsorption on the catalyst surface. Impacts of water, methanol, and hexadecane solvents on the individual steps of phenol hydrodeoxygenation are investigated over Pd/C or HZSM-5 catalyst at 473 K in the presence of hydrogen. Hydrodeoxygenation of phenol to cyclohexane includes four individual steps of phenol hydrogenation to cyclohexanone on Pd/C, cyclohexanone hydrogenation to cyclohexanol on Pd/C, cyclohexanol dehydration to cyclohexene on HZSM-5, and cyclohexene hydrogenation to cyclohexane on Pd/C. Methanol provides an additional acetal reaction route of cyclohexanone with methanol during phenol hydrodeoxygenation, compared to water and hexadecane. The hydrogenation reactions, especially of phenol

and cyclohexanone, show lower rates in methanol than in water or hexadecane. Methanol not only strongly solvates phenol and cyclohexanone but also adsorbs strongly on Pd. This strong adsorption either prevents phenol/cyclohexanone from from interacting with Pd active sites or reduces the phenol/cyclohexanone coverage coverage on the Pd/C surface, affording slower phenol/cyclohexanone hydrogenation in methanol. The low solubility of phenol and strong interaction of hexadecane–Pd surface in hexadecane lead to the slow hydrogenation rate.

The apparent activation energies for hydrogenation show the order $E_{a\ \text{phenol hydrogenation}} > E_{a\ \text{cyclohexanone hydrogenation}} > E_{a\ \text{cyclohexene hydrogenation}}$, and the reaction rates follow $\text{TOF}_{\text{cyclohexene hydrogenation}} > \text{TOF}_{\text{cyclohexanone hydrogenation}} > \text{TOF}_{\text{phenol hydrogenation}}$ at 473 K. The in situ liquid IR spectroscopy results confirm that the rates are consistent with kinetics derived from chromatographic evidence in the aqueous phase and verify that hydrogenation of phenol and cyclohexanone follows reaction orders of 1.0 and 0.55 over Pd/C, respectively. Conversion of cyclohexanol with HZSM-5 shows first-order dependence in the dehydration–hydration equilibrium. The dehydration rates and apparent activation energies are comparable in three solvents. The control of the balance between metal and acid sites is crucial to optimize the cascade reactions consisting of the integrated hydrogenation and dehydration steps, which allows developing active and stable catalysts.

Acknowledgments

J.H. gratefully acknowledges the support of the TUM graduate school's faculty graduate center of chemistry (FGCh) at the Technische Universität München, the Elitenetzwerk Bayern (graduate school NanoCat). (graduate school NanoCat). M.Sc. Stanislav Kasakov is acknowledged for fitting the experimetal data of overall phenol hydrodeoxygenation. C.Z. thanks the support from European Graduate School for Sustainable Energy. J.A.L. acknowledges the support from the US Department of Energy, Office of Basic Energy Sciences. Pacific Northwest National Laboratory (PNNL) is a multiprogram national laboratory operated for DOE by Battelle.

Appendix A. Supplementary material

Supplementary data associated with this article can be found, in the online version, at http://dx.doi.org/10.1016/j.jcat.2013.09.009.

References

[1] E. Furimsky, Appl. Catal. A 199 (2000) 147.
[2] C. Zhao, Y. Kou, A.A. Lemonidou, X. Li, J.A. Lercher, Angew. Chem. Int. Ed. 48 (2009) 3987.
[3] C. Zhao, J.A. Lercher, Angew. Chem. Int. Ed. 51 (2012) 5935.
[4] C. Zhao, J. He, A.A. Lemonidou, X. Li, J.A. Lercher, J. Catal. 280 (2011) 8.
[5] C. Zhao, D.M. Camaioni, J.A. Lercher, J. Catal. 288 (2012) 92.
[6] C. Zhao, J.A. Lercher, ChemCatChem 4 (2012) 64.
[7] J. He, C. Zhao, J.A. Lercher, J. Am. Chem. Soc. 134 (2012) 20768.
[8] J.S. Shabtai, W.W. Zmierczak, E. Chornet, US Patent, The University of Utah Research Foundation, 6,172,272 B1, 2001.
[9] C.-L. Li, Z.-R. Xu, Z.-A. Cao, B.C. Gates, AIChE J. 31 (1985) 170.
[10] Y.Q. Yang, C.T. Tye, K.J. Smith, Catal. Commun. 9 (2008) 1364.
[11] L.R. Snyder, J. Chromatogr. 92 (1974) 223.
[12] U.K. Singh, M.A. Vannice, Appl. Catal. A 213 (2001) 1.
[13] M. Boudart, D.J. Sajkowski, Faraday Discuss. 92 (1991) 57.
[14] Y. Xiang, L. Ma, C. Lu, Q. Zhang, X. Li, Green Chem. 10 (2008) 939.
[15] J.S. Shabtai, W.W. Zmierczak, E. Chornet, US Patent, The University of Utah Research Foundation, 5,959,167, 1999.
[16] N.M. Bertero, A.F. Trasarti, C.R. Apesteguia, A.J. Marchi, Appl. Catal. A 394 (2011) 228.
[17] N. Mahata, K.V. Raghavan, V. Vishwanathan, Catal. Today 49 (1999) 65.
[18] B.A. Sexton, K.D. Rendulic, A.E. Hughes, Surf. Sci. 121 (1982) 181.
[19] Y. Morikawa, H. Ishii, K. Seki, Phys. Rev. B 69 (2004) 041403.
[20] S. Andersson, C. Nyberg, C.G. Tengstål, Chem. Phys. Lett. 104 (1984) 305.
[21] H.A. Pray, C.E. Schweickert, B.H. Minnich, Ind. Eng. Chem. 44 (1952) 1146.
[22] A. Drelinkiewicza, A. Waksmundzka, W. Makowski, J.W. Sobczak, A. Król, A. Zieba, Catal. Lett. 94 (2004) 143.
[23] K.A. Manbeck, N.E. Musselwhite, L.M. Carl, C.A. Kauffman, O.D. Lyons, J.K. Navin, A.L. Marsh, Appl. Catal. A 384 (2010) 58.
[24] B. Peng, C. Zhao, I. Mejía-Centenoa, G.A. Fuentesa, A. Jentys, J.A. Lercher, Catal. Today 183 (2012) 3.
[25] R. Krishna, J.M. van Baten, Langmuir 26 (2010) 10854.
[26] J. Macht, M.J. Janik, M. Neurock, E. Iglesia, Angew. Chem. Int. Ed. 46 (2007) 7864.
[27] H. Noller, W. Kladnig, Catal. Rev. 13 (1976) 149.
[28] T. Xu, J.F. Haw, J. Am. Chem. Soc. 116 (1994) 7753.
[29] G. Odian, Principles of Polymerization, fourth ed., Wiley-Interscience, Hoboken, NJ, 2004.
[30] J.M.G. Cowie, V. Arrighi, Polymers Chemistry and Physics of Modern Materials, third ed., Taylor & Francis, Boca Raton, 2008.
[31] E.E. Gonzo, M. Boudart, J. Catal. 52 (1978) 462.
[32] F. Kapteijn, J.A. Moulijn, R.A. van Santen, R. Wever, Stud. Surf. Sci. Catal. 123 (1999) 81.
[33] N. Mahata, V. Vishwanathan, J. Mol. Catal. A 120 (1997) 267.
[34] H. Knözinger, K. Kochloef, H. Bühl, J. Catal. 24 (1972) 57.
[35] C. Zhao, Y. Yu, A. Jentys, J.A. Lercher, Appl. Catal. B 132–133 (2013) 282.
[36] C. Zhao, S. Kasakov, J. He, J.A. Lercher, J. Catal. 296 (2012) 12.
[37] R. West, J. Am. Chem. Soc. 81 (1959) 1614.